

CrossMark
click for updatesCite this: *RSC Adv.*, 2017, 7, 3376

Assessment of structural characteristics of regenerated cellulolytic enzyme lignin based on a mild DMSO/[Emim]OAc dissolution system from triploid of *Populus tomentosa* Carr.†

Tian-Ying Chen,^a Bing Wang,^a Xiao-Jun Shen,^a Han-Yin Li,^a Yu-Ying Wu,^a Jia-Long Wen,^{*a} Qiu-Yun Liu^b and Run-Cang Sun^a

The structural characteristics of native lignin are essential for the further deconstruction of plant cell walls for value-added application of lignocellulosic biomass. An improved protocol of cellulolytic enzyme lignin named regenerated cellulolytic enzyme lignin (RCEL) was developed in the present study. The dissolution process of poplar wood in the DMSO/[Emim]OAc dissolution system was dynamically monitored by microscopes and Confocal Raman Microscopy (CRM). The yield of RCEL (43.0–85.3%) was significantly higher than that of control CEL (30.6%). The isolated lignins were elaborately characterized by associated carbohydrates, 2D-HSQC NMR, ³¹P-NMR, and GPC techniques. NMR results showed that RCELs had similar structural features as compared to CELs. The relative abundances of the major lignin linkages (β -O-4', β - β' , β -5', and β -1') and linked molecules (*p*-hydroxybenzoate) were quantitatively compared. Subsequent CP/MAS ¹³C-NMR spectra of the regenerated substrates demonstrated that the structural changes of the cellulose in the substrates occurred during the dissolution and regeneration process, resulting in efficient enzymatic hydrolysis (63.2–88.7% vs. 49.5%), thus obtaining a high yield of extracted lignin (RCEL). In short, the understanding of native lignin in fast-growing poplar will contribute to the diversification of the biomass feedstock supply for designing effective deconstruction strategies for lignocellulosic biomass.

Received 22nd October 2016
Accepted 20th December 2016

DOI: 10.1039/c6ra25663e

www.rsc.org/advances

1. Introduction

Lignocellulosic biomass is attracting lots of attention due to its potential as an abundant renewable resource, it could replace fossil fuels as the major feedstock for the production of fuels, chemicals, and materials.¹ Biomass deconstruction is a crucial step to realize the value-added applications of this abundant renewable resource. Among the various factors affecting biomass deconstruction, the presence of lignin is one of the most significant reasons for biomass recalcitrance.² In general, the effective dissociation of lignin from plant cell wall mainly depends on the understanding of structural characteristics of

native lignin in the plant and developing an appropriate separation strategy. Therefore, better understanding of chemical composition and structural characteristics of native lignin is of vital importance for the further deconstruction of plant cell wall for value-added application of lignocellulosic biomass.

In the plant cell wall, lignin is the most abundant natural aromatic polymer second to cellulose, and regarded as being formed by three hydroxycinnamyl alcohol according to degree of methoxylation: *p*-coumaryl, coniferyl, and sinapyl alcohols.³ These monolignols generate different types of lignin units, such as H (*p*-hydroxyphenyl), G (guaiacyl), and S (syringyl) units. Although the structure of the lignin has been studied for many years, its complexity and irregularity have not yet been completely elucidated due to the current cognitive level.³ In fact, the understanding of the structure of lignin mainly depends on the constantly progressive lignin extraction and analysis technologies although some key substructures are identified and characterized by pioneers.³ Meanwhile, the structural substructures of lignin in the plant cell wall can be also characterized by the *in situ* whole cell wall NMR techniques.^{4–6} However, *in situ* whole cell wall NMR techniques usually need higher configuration of equipments, such as cryogenic NMR probe and nuclear magnetic field intensity (more than 400

^aBeijing Key Laboratory of Lignocellulosic Chemistry, Beijing Forestry University, Beijing, 100083, China. E-mail: wenjialonghello@126.com; wenjialong@bjfu.edu.cn; Fax: +86-10-62336903; Tel: +86-10-62336903

^bThe Biocomposites Centre, Bangor University, Bangor, UK

† Electronic supplementary information (ESI) available: Table S1. Quantification of crystallinity index in the raw and regenerated poplar wood by CP/MAS ¹³C NMR. Table S2. Assignments of ¹³C-¹H correlation signals in the HSQC spectra of the lignin from poplar wood. Fig. S1. Dissolution of ball-milled wood in DMSO/[Emim]OAc solvent system under different temperatures (optical microscope). Fig. S2. ³¹P-NMR spectra of the lignin fractions isolated from poplar wood. Additionally, parts of "Methods" in Experimental section were also supplemented. See DOI: 10.1039/c6ra25663e



MHz), restricting its applications in regular laboratory regarding to wood chemistry. In addition, to obtain more detailed structural characteristics of lignin macromolecule in the plant cell wall, lignin extraction by neutral solvent (*i.e.* dioxane) is usually highly needed. In general, it is vital important to obtain a more representative lignin sample prior to analyzing the structural features of lignin in the plant cell wall. However, a principal question in elucidating the structure of native lignin is that it cannot be isolated without any chemical and physical alteration form.⁵ Björkman (1956) presented a representative MWL (milled wood lignin), in which it was extracted with aqueous dioxane (96%) from the ball-milled wood.⁷ MWL is considered to be the first main advance towards isolating lignin in a relatively unaltered state. By contrast, other methods used enzymatic treatment to remove the majority of carbohydrates, prior to solvent extraction with aqueous dioxane, producing a relatively higher yield of lignin called cellulolytic enzyme lignin (CEL).⁸ However, it takes a long time to obtain CEL, and the yields (more than 30%, based on the total amount of lignin) are often related to ball-milling process and subsequent purification process. In fact, the yield of CEL is mostly ascribed to the existence of highly crystalline and inaccessible cellulose, which is also embedded in a matrix of wood polysaccharides and lignin.⁹ Ball-milling process facilitates the disintegration of crystalline structures of cellulose, but the dissolution or swelling of ball-milled biomass by specific solvents was considered to be a more facile method for disrupting the crystalline structure of cellulose and increasing its accessibility to cellulases.^{10,11} Thus, the efficiency of enzymatic hydrolysis of cellulose in different pretreated substrates can be improved to different degrees after different dissolution or swelling process.

Fortunately, the knowledge of plant cell wall dissolution systems facilitates the development of new methods for lignin isolation. Zhang *et al.*, (2010) had proposed a modified CEL method with a higher yield (45.8%) as compared to corresponding CEL (36.5%) based on DMSO/*N*-methylimidazole dissolution system.¹¹ Afterwards, Capanema *et al.* (2014) had developed a novel lignin isolation method, in which the ball-milled lignocellulose was dissolved in DMSO/LiCl solvent system and then regenerated it in water prior to enzymatic hydrolysis.¹² The lignin obtained was named as regenerated cellulolytic enzyme lignin (RCEL). It was also found that the yield of RCEL extracted with 80% aqueous dioxane from 3 h ball-milled hardwood reached to 93%,¹² which was higher than that (70%) of corresponding CEL-80%. Similarly, it was found that the yield of RCEL extracted with 96% dioxane from the regenerated substrates based on DMSO/LiCl solvent system reached 73.2% (based on Klason lignin in original internode from wheat straw), which was slightly higher than that of corresponding CEL (68.2%).¹³ Recently, DMSO-*d*₆ and [Emim]OAc-*d*₁₄ were used to dissolve *Miscanthus* cell walls, aiming to *in situ* characterize the structural features of lignin in *Miscanthus* by 2D-HSQC technique.¹⁴ However, the signals representing for lignin substructures in *in situ* 2D-HSQC spectra of the whole cell wall were hindered by other signals of carbohydrates, especially for the signals of acylation in some hardwood (poplar wood and

willow), in addition, some deuterated solvents (*e.g.* deuterated ionic liquid) were currently unavailable although they have a good dissolving capacity for fine ball-milled plant cell wall. Because of good dissolving capacity of DMSO and [Emim]OAc to ball-milled plant cell wall, thus it can be used for regenerating plant cell wall prior to enzymatic hydrolysis, aiming to increase the enzymatic hydrolysis efficiency.

Triploid of *Populus tomentosa* Carr., a kind of fast-growing poplar species widely planted in China due to its large quantity and various beneficial characteristics, such as cold resistance, drought tolerance, and pest resistance.¹⁵ Moreover, this new variety is superior in short rotation and high wood quality to other poplar varieties. To effectively isolate a more representative native lignin and understand the molecular characteristic of lignin as well as lignin-carbohydrate complex in this kind of poplar wood, the mixture of DMSO and [Emim]OAc at different temperatures was used to dissolve the plant cell wall prior to enzymatic hydrolysis and the dissolution behavior of the lignocelluloses was revealed by the fluorescence microscope and confocal Raman spectroscopy. Afterwards, 80% aqueous dioxane was used to extract RCEL-80% from the regenerated cell wall after enzymatic hydrolysis, and the yields, associated carbohydrates (also lignin-carbohydrate complexes, LCC), molecular weights (gel permeation chromatography, GPC), structural characteristics (2D heteronuclear single quantum coherence, 2D-HSQC), and functional groups (³¹P-NMR) of the isolated native lignin were comprehensively investigated as compared to those of traditional CEL sample. Furthermore, the structural changes of the regenerated substrates obtained after the dissolution and regeneration process were characterized by solid-state CP/MAS ¹³C-NMR spectroscopy and the glucose released from enzymatic hydrolysis of the substrates was also evaluated by the high performance anion exchange chromatography (HPAEC). It is believed that the proposed lignin isolating method will improve the understanding of lignin-lignin and lignin-carbohydrate linkages in the plant cell wall of this fast-growing poplar, which will enable the development of a more efficient deconstruction strategy for the poplar wood.

2. Experimental section

2.1. Materials

Poplar wood (triploid of *Populus tomentosa* Carr.), which is 5 year-old was taken from Shandong province in China, in March, 2015, removed the bark and then ground using a Wiley Mill to pass a 20–40 mesh sieve. The subsequent treatment with a mixture of ethanol/benzene (1 : 2, v/v) for 6 h removed extractives and obtained extractives-free samples. The dewaxed samples were air-dried at 60 °C for 16 h and stored at 5 °C before use. The major components (% w/w) of the poplar wood were cellulose (45.82%), hemicelluloses (21.00%), and lignin (22.78%) based on a dry weight basis, respectively, which were analyzed by the standard of National Renewable Energy Laboratory (NREL).¹⁶ The dewaxed wood powder (25 g) was subjected to milling in a planetary ball mill (Fritsch GmbH, Idar-Oberstein, Germany) at a fixed frequency of 500 rpm for 5 h under N₂ (room temperature) as previously.¹⁷ All chemicals used



in this study were purchased from Sigma Chemical Co. (Beijing, China), except for cellulase.

2.2. Dissolution and regeneration of ball-milled poplar wood

The solvent of 2% DMSO/[Emim]OAc was prepared by dissolving 2 mL of [Emim]OAc in 98 mL DMSO. The ball-milled poplar wood (10 g) was suspended into the prepared 400 mL 2% DMSO/[Emim]OAc solvent system. Dissolution process was performed at 60, 80, and 100 °C for 2 h, respectively. A drop of mixture was taken out every 30 min in the dissolution process and placed onto a glass slide to make a cross section. Other wood samples could be completely regenerated by adding the dissolved wood sample to about 3 volumes of deionized water, then centrifuging and washing. The regenerated sample was further freeze-dried for further treatment. Meanwhile, poplar wood section about 8 μm thickness was treated according to the methods aforementioned.

2.3. Isolation of cellulolytic enzyme lignin (CEL) and regenerated cellulolytic enzyme lignin (RCEL)

CEL preparation is one of the well-established methods to isolate lignin for structural elucidation.⁸ Technically, the CEL and RCEL samples were prepared as the following procedures, the ball-milled material (10 g) or the regenerated materials (8.23–9.10 g) were suspended in acetate buffer (0.05 mol l⁻¹, pH 4.8), and the substrate concentration was about 5%. Then cellulase (Cellic@ CTec2, 100 FPU mL⁻¹), which was kindly provided from Novozymes, Beijing, China, was added into the suspension with 50 FPU g⁻¹ substrate, prior to incubating in a shaker (180 rpm) (DZH-2102, Jinghong, Shanghai, China) at 50 °C for 72 h. After enzymatic hydrolysis, the mixtures were centrifuged to remove the supernatant after enzymatic hydrolysis, the residues were washed for 2–3 times using acetate buffer and deionized water, respectively, and then freeze-dried. The dried enzymatic hydrolyzed samples were extracted (2 \times 24 h) with 96% and 80% aqueous dioxane (v/v) with a solid to liquid ratio of 1 : 40 (g mL⁻¹). By contrast, the enzymatic hydrolysis residues of regenerated wood were extracted with 80% aqueous dioxane with a solid to liquid ratio of 1 : 40 (g mL⁻¹) at room temperature for 48 h (2 \times 24 h). The extracting liquid, which were obtained by centrifugation, were concentrated and precipitated into 10 volumes of acid water (pH = 2.0), then the precipitated lignin were freeze-dried to obtain crude CEL and RCEL samples. To remove some carbohydrates remained in these preparations, purification was necessary. The crude CEL and RCEL samples (1 g) were dissolved into 20 mL 90% acetic acid and removed the insoluble part, the supernatants were slowly dropped into 10 volumes of acid water (pH = 2.0) and washed several times with deionized water. The residues were freeze-dried and then the purified lignin samples were obtained. Meanwhile, to understand the differences in yield of RCEL samples under different dissolution temperatures, it is important to acquire the curves regarding to glucose yield *versus* time at different temperatures, *i.e.* enzymatic hydrolysis efficiency. The procedure of enzymatic hydrolysis is in accordance with the aforementioned method, except for the

doses of cellulase (15 FPU g⁻¹ substrate for enzymatic hydrolysis efficiency), during the process, the hydrolysates were termly sampled (3, 6, 9, 12, 24, 48, 60, 72 h) and analyzed by a HPAEC (Dionex, ICS 3000, U.S.) system.

2.4. Characterization of ball-milled and regenerated ball-milled poplar wood

Composition analysis was conducted by hydrolyzing the extractives-free poplar wood and lignin preparations with dilute sulfuric acid according to the NREL protocol.¹⁶ The acid-soluble lignin was measured by absorbance at 240 nm in a UV-vis spectrometer (TU-1810, Beijing, China). The structural changes of the regenerated substrates obtained during the dissolution process were characterized by solid-state CP/MAS ¹³C-NMR spectroscopy, and the enzymatic hydrolysis of the substrates was also evaluated by the high performance anion exchange chromatography (HPAEC).

To detect the change of poplar wood during dissolution process, microscope (Optical Microscope Nikon eclipse E200 and Fluorescence Microscope LEICA DM 2500) and Confocal Raman Microscopy (CRM) were combined to achieve this purpose. Confocal Raman Microscope (Horiba Jobin Yvon, Longjumeau, France) is a LabRam XploRa equipped with a confocal microscope (Olympus BX51, Tokyo, Japan) and a motorized x, y stage. The high spatial resolution of confocal Raman microscopy was ascribed to an MPlan 100 \times oil immersion microscope objective (Olympus, NA = 1.40) and a linear-polarized laser (532 nm), which possessed of a diffraction-limited spot about 1.22/NA. An air-cooled back-illuminated CCD behind the spectrograph was used to detect the Raman light. The detail method of making up cross section was followed the pattern as previously.¹⁸ The spectra were extracted from the secondary wall (S) and cell corner middle lamella (CCML) of the fiber, respectively. Hence, the morphology and distribution of compositions were clearly observed along the prolongation of time.

2.5. Structure elucidation of CELs and RCELs

The weight average (M_w) and number-average (M_n) molecular weights of the lignin preparations were determined by gel permeation chromatography (GPC, Agilent 1200, USA) according to a previous publication.¹⁹ In general, acetylation process is necessary for measuring molecular weights of the native lignin samples. The detailed procedure of acetylation is revealed in the ESI[†] 2D-HSQC NMR and ³¹P-NMR spectra were recorded on a Bruker AVIII 400 MHz spectrometer at 25 °C in DMSO-d₆ fitted with a 5 mm gradient probe with inverse probe. For 2D-HSQC spectra, 50 mg of lignin was dissolved in 0.5 mL of DMSO-d₆, and the sequence was conducted according to literature method (ESI[†]).¹⁹ The quantitative ³¹P-NMR spectra of CEL and RCEL samples were acquired after the reaction of lignin with 2-chloro-4,4,5,5-tetramethyl-1,3,2-dioxaphospholane (TMDP) according to a previous literature.²⁰ All experiments in this study were performed in duplicate, and the data reported were the average values.



3. Results and discussion

3.1. Dissolution of ball-milled wood in DMSO/[Emim]OAc solvent system

The optical microscope was used to observe the dissolution process of DMSO/[Emim]OAc solvent system under different pretreatment temperatures. As shown in Fig. S1,[†] it was found that the ball-milled poplar wood could be mostly dissolved at 80 and 100 °C for 2 hours. Accordingly, pretreatment temperatures at 80 and 100 °C will be beneficial to the regeneration and subsequent enzymatic hydrolysis process of the substrates.

To reveal the microscopic distribution and change of lignin in the poplar cell walls before (raw) and after dissolution process pretreatments at different temperatures (60, 80, and 100 °C), the poplar cell wall slices were subjected to the fluorescence microscope to trace these changes. As shown in Fig. 1, the fluorescence intensity of raw poplar wood was weak, while those for the pretreated cell walls slices were progressively increased with the pretreatment temperatures, especially at 100 °C. Additionally, the fluorescence intensity was also enhanced with the prolongation of pretreatment times. This phenomenon suggested that increasing content of lignin fractions dissolved during the pretreatment process were reprecipitated onto the surface of plant cell walls during the regeneration process.

3.2. Confocal Raman microscopy analysis

Raman images of lignin and carbohydrate distribution in the control and regenerated poplar wood cell walls are shown in Fig. 2. In the Raman images, the varying intensity reflected the different concentrations of lignin (left column) and carbohydrate (right column) in morphologically distinct cell wall

regions. For the control poplar wood, the highest concentration of lignin was found in the cell corner middle lamella (CCML) regions, followed by compound middle lamella (CML), and the lowest level of intensity was in the secondary (S) regions. After the dissolution process of DMSO/[Emim]OAc solvent system under different temperatures, the concentrations of lignin in the pretreated samples showed a decreased trend in different degrees. In addition, the lignin concentrations in CCML and CML were obviously weakened after the dissolution process at 80 °C and 100 °C. Moreover, the intermittent distribution of lignin was also observed after dissolution process at 80 °C and 100 °C, suggesting that the relatively higher solution temperature will lead to the re-arrangement of lignin in the plant cell wall. In fact, the redistribution of lignin in plant cell wall means that the morphological and structural features of carbohydrates also changed during the dissolution process, which would finally change the digestibility of plant cell wall. By contrast, the concentration of carbohydrates in the plant cell wall increased after the dissolution process, especially at 80 °C, implying that the lignin was mostly removed from the CCML and CML by DMSO/[Emim]OAc solvent system under the conditions given.

3.3. Chemical and structural characterization of ball-milled and regenerated ball-milled poplar wood as well as corresponding enzymatic hydrolysis

To investigate the effect of DMSO/[Emim]OAc dissolution process on the recovery yield and chemical composition of poplar wood, the absolute component analysis of raw material and the pretreated substrates were measured. As shown in Table 1, the recovery yield of the ball-milled poplar under 60, 80, and 100 °C was 87.9, 91.0, and 82.3%, respectively. For raw poplar wood, the weight of hemicelluloses (including

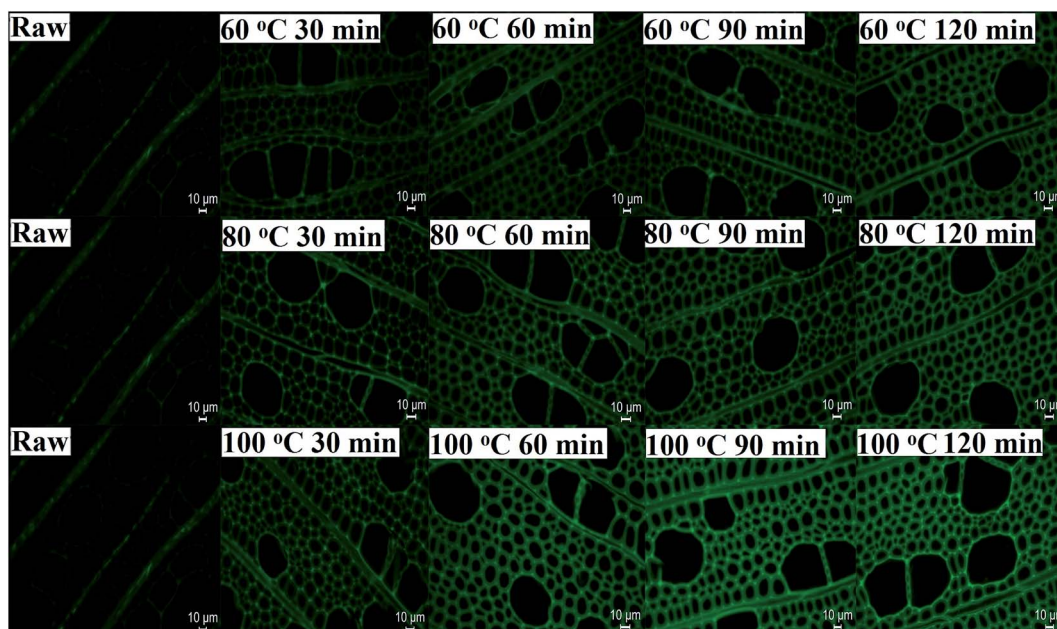


Fig. 1 Fluorescence microscope photos of poplar cell walls before (raw) and after dissolution treatments at different temperatures (60, 80, and 100 °C).



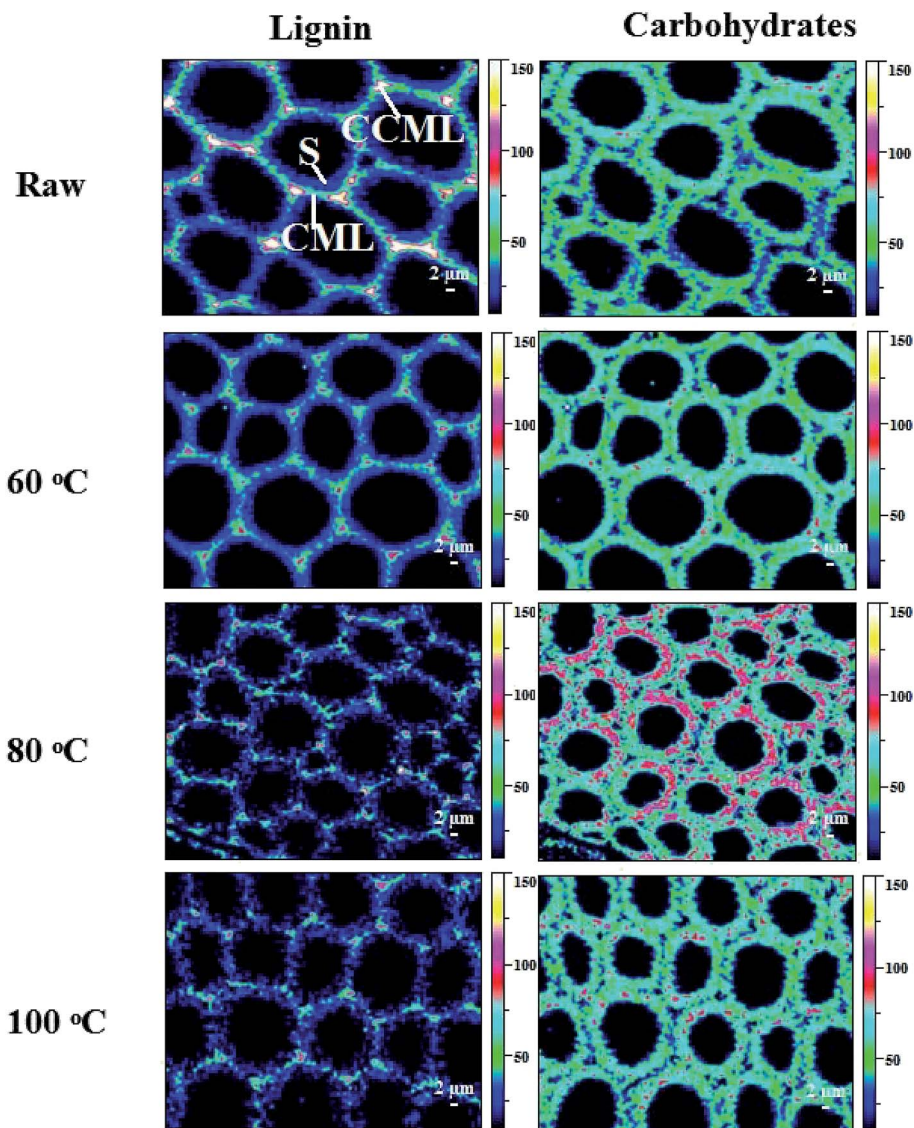


Fig. 2 Raman images of the lignin and carbohydrates distributions in raw and the regenerated samples at different dissolution temperatures.

Table 1 Composition analysis of the raw and regenerated ball-milled poplar under different temperatures

Samples	Recovery yield ^a (%)	Rha ^b	Ara ^b	Gal ^b	Xyl ^b	Man ^b	Uronic acid	Glu ^b	AL ^c	KL ^d	Total (%)
Raw	100.0	0.50	0.28	0.72	16.7	1.99	0.87	45.80	0.98	21.80	89.64
R-Raw-60 °C	87.9	0.40	0.26	0.47	16.4	1.27	0.80	44.60	1.09	19.15	84.44
R-Raw-80 °C	91.0	0.30	0.23	0.44	14.4	1.06	1.06	44.20	1.43	16.87	79.99
R-Raw-100 °C	82.3	0.20	0.19	0.38	13.2	1.20	0.91	44.80	0.98	15.43	77.29

^a Based on 100 g of ball-milled poplar wood. ^b Rha, rhamnose; Ara, arabinose; Gal, galactose; Xyl, xylose; Man, mannose; Glu, glucose. ^c Acid-soluble lignin. ^d Klason lignin.

rhamnose, arabinose, galactose, xylose, mannose, and uronic acid) in 100 g wood was 21.06 g, while it was decreased to 19.60, 17.49, and 16.08 g under the dissolution temperatures of 60, 80, and 100 °C, respectively. The cellulose content expressed by glucose was also decreased from 45.80 to 44.20 g after the dissolution process. It should be mentioned that some lignin fragments released during ball-milling process were lost in

DMSO/[Emim]OAc/water mixture system (dissolution and regeneration process), which can be seen from the decreased lignin content in Table 1. However, the amount of this part of lignin fragments is slight. In previous studies, the recovery yields of regenerated wood in different dissolution system were not mentioned, such as DMSO/NMI¹¹ and DMSO/LiCl¹² system, but the recovery yield was mentioned in a recent publication, in



which the regenerated solid recovery was decreased from 91 to 85% as the milling time prolonged from 2 to 6 h.¹³ In fact, the loss of lignin is overvalued based on the Table 1 in this study. As can be seen from CP/MAS spectra of the regenerated poplar substrates, the signal for DMSO was found at 39.5 ppm in the spectra of R-raw-100 °C, suggesting that a trace amount of residual DMSO (39.5 ppm) still remains in the substrates, which will affect the compositional analysis of the regenerated substrate. However, in this study, the optimal dissolution temperature of DMSO/[Emim]OAc is 80 °C under the conditions given, which was used for regenerating the plant cell wall and further RCEL extraction. In this case, lignin loss is less than that calculated from Table 1.

The CP/MAS ¹³C-NMR spectra (Fig. 3) evidenced that DMSO/[Emim]OAc solvent system resulted in structural changes of crystalline region of the ball-milled poplar wood. For raw ball-milled poplar wood, the crystallinity index (CrI) was 19.68%, while the CrI for the regenerated substrates (R-raw-60 °C, R-raw-80 °C, and R-raw-100 °C) was 24.10%, 26.26%, and 21.36%, respectively (Table S1†). The firstly increased CrI of the substrates was probably attributable to the removal of

hemicelluloses and lignin, which were deemed as amorphous substances in the plant cell wall.^{10,11} However, the decreased CrI for R-raw-100 °C was observed, suggesting that the partial degradation of crystalline region in cellulose also occurred during the dissolution and regeneration process at the high temperature (100 °C). Besides the structural changes of cellulose, the relatively unchanged signal for lignin (151.98 ppm, etherified S_{3,5}) suggested that the main structures of lignin remain unchanged during the dissolution and regeneration process. Similarly, the appearance of the signals for acetyl groups (20.23 and 171.17 ppm) in hemicelluloses also implied that no obvious structural changes of hemicelluloses occurred during the process. Although the plant cell wall was subjected to ball-milling, the cellulose in plant cell wall is partly crystalline (Fig. 3), and highly inaccessible to enzymatic attack.²¹ In this study, the DMSO/[Emim]OAc solvent system was used for dissolution of the ball-milled poplar wood. The wood samples could be mostly dissolved after the dissolution process. After the regeneration, it was found that the enzymatic digestibility of the regenerated substrates (63.2–88.7%, Fig. 4) was significantly improved as compared to that of control sample (49.5%, ball-

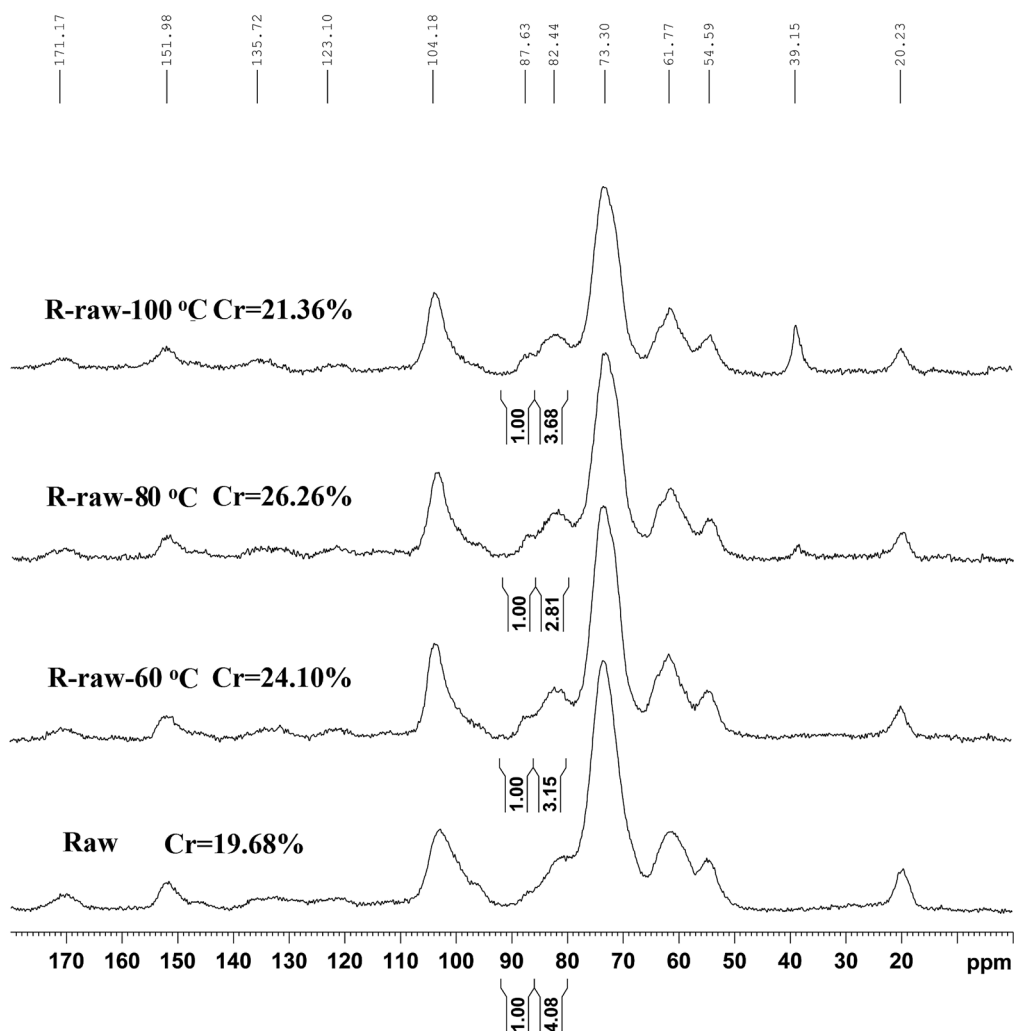


Fig. 3 CP/MAS ¹³C-NMR spectra of the raw and regenerated ball-milled poplar wood.



milled poplar wood). Obviously, the optimal enzymatic digestibility of R-raw-80 °C reached to 88.7%. However, the slightly decreased enzymatic digestibility of R-raw-100 °C was probably due to the existence of trace amount of residual DMSO (39.5 ppm) in the substrates, as also revealed by the aforementioned CP/MAS ¹³C-NMR spectra. In short, the greatly enhanced efficiency of enzymatic hydrolysis of the regenerated ball-milled wood is primarily ascribed to the deconstructed plant cell wall (migratory lignin reflected from CRM) in this solvent system.²²

3.4. Yield and carbohydrate analysis of the CELs and RCELs

Traditionally, CEL was mostly used for structural analysis of native lignin in biomass. The method uses cellulolytic enzyme mixtures (containing cellulase and hemicellulase) to remove most of the carbohydrates prior to lignin extraction with aqueous 1,4-dioxane.²³ However, the yield of CEL was only 30.6% based on the total lignin of poplar wood in the present study (Table 2). The reason for the low yield of CEL could be ascribed to the unsatisfactory enzymatic hydrolysis efficiency of the ball-milled wood. Although 80% dioxane can extract more native lignin as compared to 96% dioxane,¹⁵ the yield only increased from 30.6 to 41.3% in this study. However, most lignin macromolecule still remained in the residue after 80%

dioxane extraction. After regeneration and enzymatic hydrolysis, the yields of RCEL-80% (RCEL-60 °C, RCEL-80 °C, and RCEL-100 °C, extracted with 80% dioxane) under different dissolution conditions were increased from 43.0 to 85.3% (based on the total lignin content of regenerated wood sample). The result indicated that regeneration process prior to enzymatic hydrolysis led to disintegration of the ultramolecular structure of cellulose in the plant cell wall, improved the accessibility of cellulase to the regenerated poplar wood and increased the enzymatic hydrolysis efficiency of the regenerated poplar wood, obtained enzymatic hydrolysis residue (lignin-rich residue), and significantly enhanced the yield of RCEL samples under different dissolution conditions. It was observed that the dissolution of poplar wood under 80 °C in the presence of DMSO/[Emim]OAc led to the highest yield of RCEL, which is positively related to the highest enzymatic hydrolysis efficiency of the preswelled ball-milled poplar wood. With regarding to the carbohydrate content, the value for RCEL-80 °C was 6.96%, which was slightly higher than those of RCEL-60 °C (6.62%) and RCEL-100 °C (6.01%). By contrast, a small quantity of associated carbohydrate was also appeared in CEL-80% (5.00%) and CEL-96% (2.78%). However, it should be noted that RCEL-80 °C has the highest yield among all these CEL and RCEL samples, thus the optimal dissolution temperature of DMSO/[Emim]OAc is 80 °C under the conditions given. As for the carbohydrate composition, it was found that xylose was the major component sugar and comprised 48.2% of the total sugars in the CEL-80%, which was higher than that of CEL-96% (41.7%). Similarly, xylose was also the major sugar in RCEL-80%, reaching to 50.6% for RCEL-60 °C, 49.6% for RCEL-80 °C, 51.1% for RCEL-100 °C. For other secondary sugars, such as glucose, galactose, glucuronic acid, arabinose, mannose, and rhamnose, the relative proportion of these monosaccharides in total sugars was similar in the CEL-80% and RCEL-80% extracted with 80% dioxane, while the relative proportion of glucuronic acid and arabinose was low in CEL-96% as compared to those in CEL-80% and RCEL-80%. The results showed that the lignin released as CEL-96% in this study may contain more linear hemicelluloses (xylans), while the lignin isolated as CEL-80% and RCEL-80% probably contain more branched hemicelluloses, which was in line with a previous publication.¹⁷ Considering the different forms of associated xylan in these lignins, the presence of these carbohydrates in the isolated CEL and RCELs could be probably attributable to different xylan–lignin linkages.²⁴

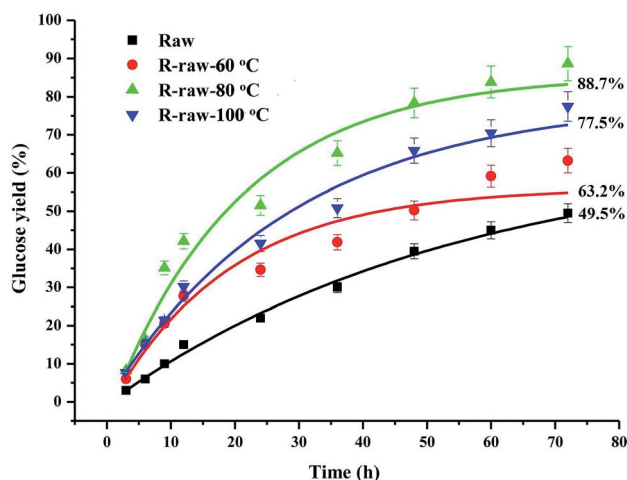


Fig. 4 Enzymatic digestibility of the raw and regenerated ball-milled poplar wood.

Table 2 Yield and carbohydrate contents of lignin samples from poplar wood

Samples	Yield (%)	Total sugars (%)	Carbohydrate content (%)						
			Rha ^b	Ara ^b	Gal ^b	Glu ^b	Xyl ^b	Man ^b	GluA ^b
CEL-96%	30.6	2.78	0.27	0.08	0.35	0.70	1.16	0.14	0.07
CEL-80%	41.3	5.00	0.51	0.26	0.43	0.82	2.41	0.31	0.28
RCEL-60 °C ^a	43.0	6.62	0.36	0.46	0.78	0.77	3.35	0.41	0.49
RCEL-80 °C ^a	85.3	6.96	0.39	0.48	0.93	0.68	3.45	0.44	0.58
RCEL-100 °C ^a	71.3	6.01	0.33	0.43	0.84	0.58	3.07	0.34	0.42

^a Extracted with 80% dioxane. ^b Rha, rhamnose; Ara, arabinose; Gal, galactose; Glu, glucose; Xyl, xylose; Man, mannose; GluA, glucuronic acid.



3.5. Molecular weight distributions

The values of the average molecular weights (M_w and M_n) and polydispersity index (M_w/M_n) of CEL and RCEL, which are calculated from the GPC curves (relative values related to polystyrene), are listed in Table 3. It was observed that CEL-80% had a highest M_w (12 870 g mol⁻¹) among all the lignin samples. As compared to CEL-80%, RCEL-80% had slightly reduced M_w (9450–12 740 g mol⁻¹). The decreased M_w of RCEL-100 °C is probably due to the slight cleavage of lignin carbohydrate and lignin–lignin linkages induced by the dissolution process. Similarly, a recent publication also demonstrated that lignin subunits after the pretreatment with [C₂mim][OAc] were released *via* depolymerization, thus leading to the reduced size and shape of the lignin.²⁵ Although the high content of associated carbohydrates will result in the augment of M_w , smaller M_w of RCEL with more carbohydrates suggested that the lignin macromolecules was probably subjected to partial depolymerization process during the dissolution process. In fact, subsequent NMR spectra of lignin would add some evidences for the decreased M_w , because that the β -O-4' linkages were slightly cleaved during the dissolution process. Similarly, it was reported that ionic liquid treatment partly destroyed the β -O-4' linkages,¹⁹ which was in agreement with the data obtained by 2D-HSQC in the present study. Moreover, all lignin fractions exhibited relatively narrow polydispersity indexes ($M_w/M_n < 2.0$), implying that these lignin fractions are relatively homogeneous molecules.

3.6. 2D-HSQC spectra analysis

To obtain the compositional and structural characteristics of the isolated CEL and RCEL, the lignin samples were elaborately analyzed using the 2D-HSQC NMR technique. The main structural characteristics of lignin, including basic composition (S, G, and H units) and various substructures linked by ether

and carbon–carbon bonds (β -O-4', β - β' , β -5', *etc.*), can be assigned in the 2D-HSQC spectra. The side-chain, aromatic regions, and anomeric regions of polysaccharides in 2D-HSQC spectra are shown in Fig. 5–7 and the main substructures are also quantified as previously²⁶ and the results are listed in Table 4.

In the side-chain regions of the spectra of poplar lignin samples, the substructures, such as β -O-4' aryl ethers (A), resinols (B), phenylcoumarans (C), could be safely assigned according to the previous publications,^{17,21,26–28} and the specific chemical shifts of the substructures are also listed in Table S2.† It was found that all the lignin samples exhibited similar spectral patterns. In the side-chain regions of 2D-HSQC spectra (Fig. 5), cross-signals of methoxyl groups (OCH₃, δ_C/δ_H 55.6/3.72 ppm) and β -O-4' ether units (substructure A) were the prominent signals. The C _{α} -H _{α} correlations in the β -O-4' linkages were observed at δ_C/δ_H 71.9/4.86 ppm, while the C _{β} -H _{β} correlations corresponding to the *erythro* and *threo* forms of the S-type β -O-4' substructures can be distinguished at δ_C/δ_H 85.8/4.11 and 86.8/3.99, respectively. The C _{β} -H _{β} correlations in structure A linked to G/H lignin units shifted to δ_C/δ_H 83.4/4.43. The C _{γ} -H _{γ} correlations in the β -O-4' substructures were detected at δ_C/δ_H 59.5/3.70 and 3.39. Additionally, the signal appearing at δ_C/δ_H 63.1/4.29 presents the C _{γ} -H _{γ} correlations in the γ -acylated lignin units (A'). Besides β -O-4' ether substructures, resinols (β - β' , substructures B) appeared in the spectra in conspicuous amounts as indicated by their C _{α} -H _{α} , C _{β} -H _{β} , and the double C _{γ} -H _{γ} correlations at δ_C/δ_H 84.8/4.65, 53.5/3.05, 71.1/3.81 and 4.17 ppm, respectively. Phenylcoumarans (β -5', substructures C) were also detected in a lower amount. Moreover, a trace amount of the spirodienone substructures (β -1', substructures D) was also detected. Furthermore, the signal located at δ_C/δ_H 61.4/4.10 is assigned to the C _{γ} -H _{γ} correlations of *p*-hydroxycinnamyl alcohol end groups (I). Besides to the common substructures, a typical lignin–carbohydrates complex (LCC) linkage has been detected, *i.e.*, benzyl-ether (BE) linkage, which was detected at δ_C/δ_H 81.0/4.65 ppm in all the spectra of CEL and RCELS. In fact, the presence of the BE linkage was also supported by the aforementioned carbohydrates analysis.

The chemical composition of the lignin (CEL and RCEL) can be revealed by the aromatic regions of the HSQC spectra (Fig. 6). The S-type lignin units showed a prominent signal for the C_{2,6}-H_{2,6} correlation at δ_C/δ_H 103.9/6.71, whereas the signal for the C _{α} -oxidized S-units (S) was observed at δ_C/δ_H 106.2/7.32. Additionally, the G-type lignin units showed different correlations for C₂-H₂ (δ_C/δ_H 110.9/6.96), C₅-H₅ (δ_C/δ_H 114.9/6.76), and

Table 3 Weight-average (M_w), number-average molecular weights (M_n), and polydispersity (M_w/M_n) of the lignin fractions isolated from poplar wood

	CEL-96%	CEL-80%	RCEL-60 °C	RCEL-80 °C	RCEL-100 °C
M_w	11 220	12 870	12 680	12 740	9450
M_n	6350	7270	7550	7660	5240
M_w/M_n	1.77	1.77	1.68	1.66	1.80

Table 4 Quantification of the lignin fractions by 2D-HSQC NMR spectra^a

Samples	S/G ^b	H _{2,6}	PB _{2,6}	β -O-4'	β - β'	β -1'	β -5'	BE	S'/(S' + S)
CEL-96%	3.08 ± 0.01	1.15 ^a	17.34	63.53	9.43	2.70	1.42	2.25	3.65
CEL-80%	3.09 ± 0.01	1.47	16.37	64.04	8.52	1.71	2.15	2.61	5.25
RCEL-60 °C	2.96 ± 0.02	1.29	14.71	59.91	10.71	1.46	0.97	3.88	4.44
RCEL-80 °C	3.41 ± 0.01	1.17	15.82	61.63	9.55	1.69	1.29	1.35	2.51
RCEL-100 °C	3.36 ± 0.01	0.99	15.55	61.05	11.63	2.99	0.46	2.06	3.51

^a Results expressed per 100 Ar based on quantitative 2D-HSQC spectra. ^b S/G ratio obtained by the this equation: S/G ratio = 0.5I(S_{2,6})/I(G₂).



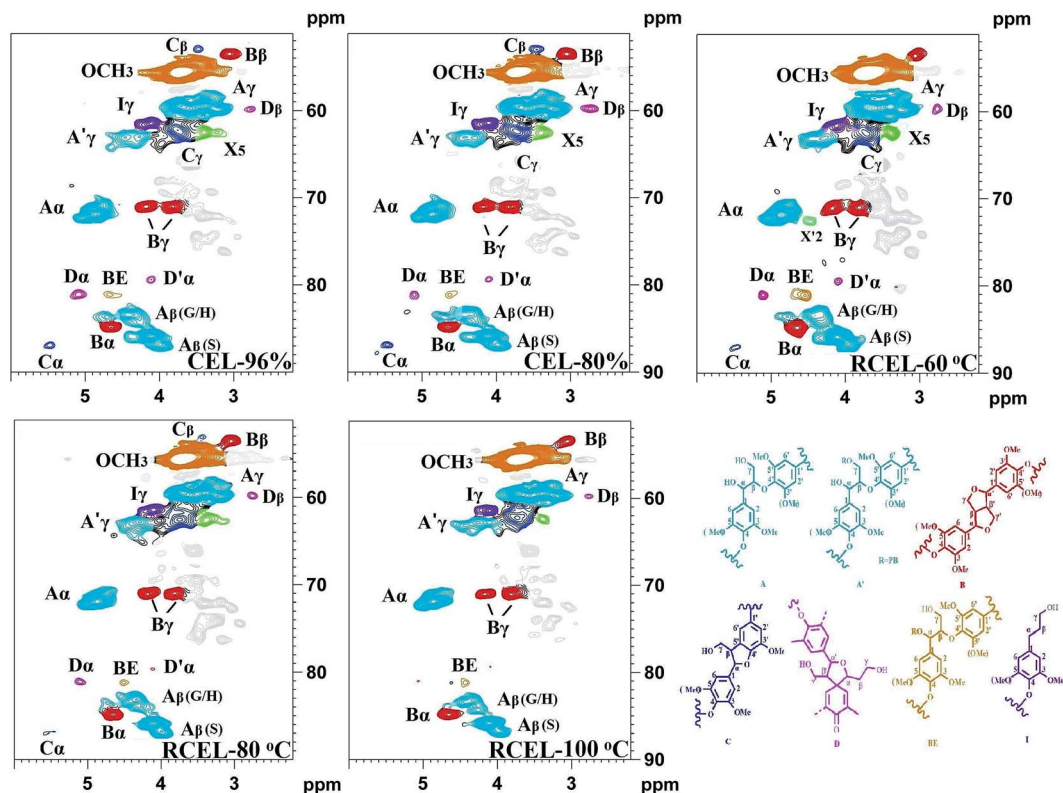


Fig. 5 2D-HSQC spectra of the lignin fractions isolated from poplar wood (side-chain region).

C_6-H_6 (δ_C/δ_H 119.0/6.78). Interestingly, small amounts of $H_{2,6}$ signals were also detected at δ_C/δ_H 127.8/7.22 ($C_{2,6}-H_{2,6}$), although its amount was low. Other significant signals in the aromatic regions of the HSQC spectra are assigned to *p*-hydroxybenzoate substructure (PB), which was observed as a strong signal at δ_C/δ_H 131.2/7.66 ($C_{2,6}-H_{2,6}$). Actually, in poplar wood, the exclusively acylated the γ -position of lignin side chains is PB, analogously with *p*-coumarates (*p*-CA) in grasses.²⁹ It was reported that γ -*p*-hydroxybenzoylated only linkages with S unit in poplar lignin and that sinapyl *p*-hydroxybenzoate is produced by enzymatic reaction and used as an authentic monomer for lignification in poplar.³⁰

The well-resolved anomeric correlations (δ_C/δ_H 90–110/4.0–5.5) of the associated carbohydrates are shown in Fig. 7. The assignments of the anomeric correlations were based on the recent publication.^{6,31} As discussed above, the corresponding anomeric correlations (C_1-H_1) of β -D-xylopyranoside units acetylated at C-2 (X_2) and C-3 (X_3) were observed at δ_C/δ_H 99.5/4.54 and 101.7/4.31, respectively. The anomeric correlations from the reducing end of (1-4)- α -D-xylopyranoside (αX_1) and (1-4)- β -D-xylopyranoside (βX_1) units were observed at δ_C/δ_H 92.2/4.88 and 97.4/4.26, respectively. Moreover, phenyl glycoside linkages (PhGlc) were also detected in the spectra of CELs and RCEL-60 °C, while the intensity of signals decreased in RCEL-80 °C and disappeared in the spectrum of RCEL-100 °C, implying that the PhGlc units were significantly cleaved in the DMSO/[Emim]OAc dissolution system at the higher temperature.

The relative abundances of the basic composition (H, G, and S lignin units), and those of the main linkages (referred to as per 100 aromatic units and as a percentage of the total side chains), calculated from the 2D-HSQC spectra of the lignin samples based on a previous publication,³² are shown in Table 4. The S/G ratio of lignin is important to evaluate the delignification process of lignocellulosic biomass. In this study, the S/G ratio of CEL-96% and CEL-80% was 3.08 and 3.09, suggesting that different concentrations of aqueous dioxane have no obvious effect on the S/G ratio of the lignin. By contrast, S/G ratio decreased slightly to 2.96 in RCEL-60 °C, and then respectively elevated to 3.41 and 3.36 in RCEL-80 °C and RCEL-100 °C, suggesting that the lignin fractions obtained can better represent the native lignin in the plant cell wall because of high S/G ratio and high yield of the lignin fractions. However, the S/G ratios (2.96–3.41) of the lignin fractions obtained in the present study were obviously higher than that (S/G = 2.29) of CEL from poplar wood previously reported.¹⁵ In fact, high S/G ratio of lignin in this study was positively related to the higher yields of lignin obtained because that the lower yield of CEL suggested that the lignin isolated with low yield may mainly originated from lignin fractions in middle lamella,³³ in which it contains fewer methoxyl groups per C9 than that in the secondary wall.³⁴

The quantification of β -O-4', β - β ', β -5', and β -1' linkages suggested that the content of β -O-4' linkages slightly decreased during the dissolution process, while the content of other linkages remained relatively unchanged. However, the content



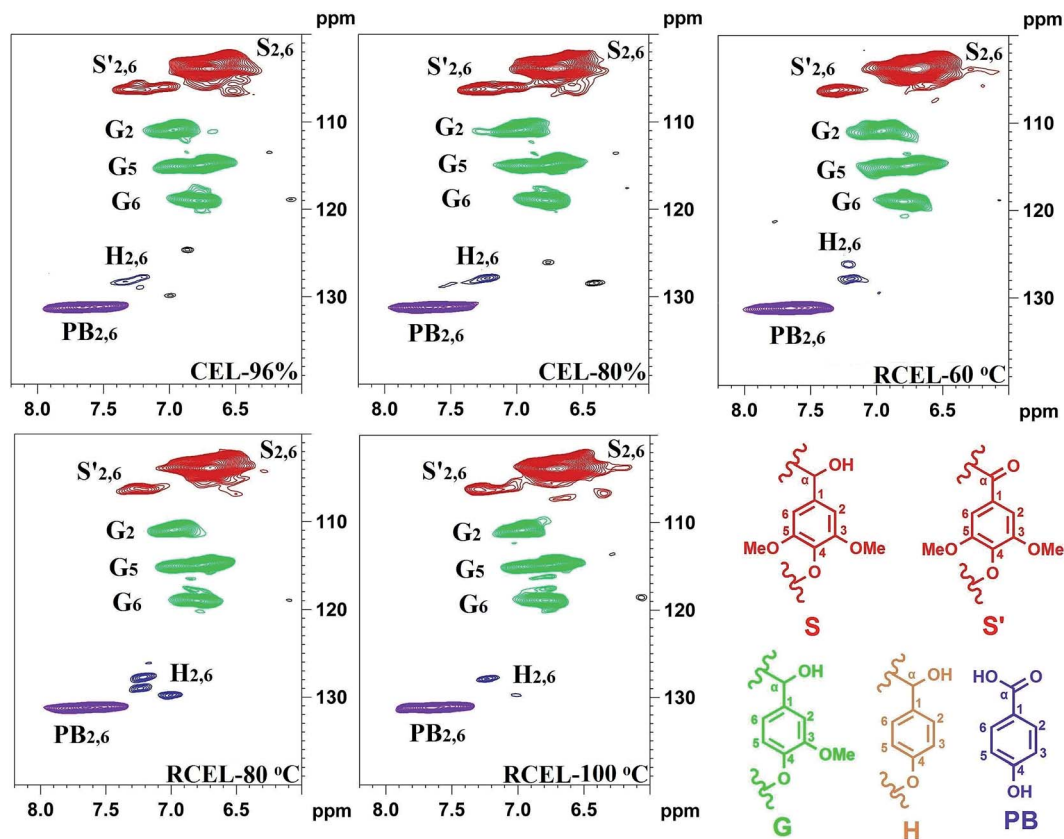


Fig. 6 2D-HSQC spectra of the lignin fractions isolated from poplar wood (aromatic region).

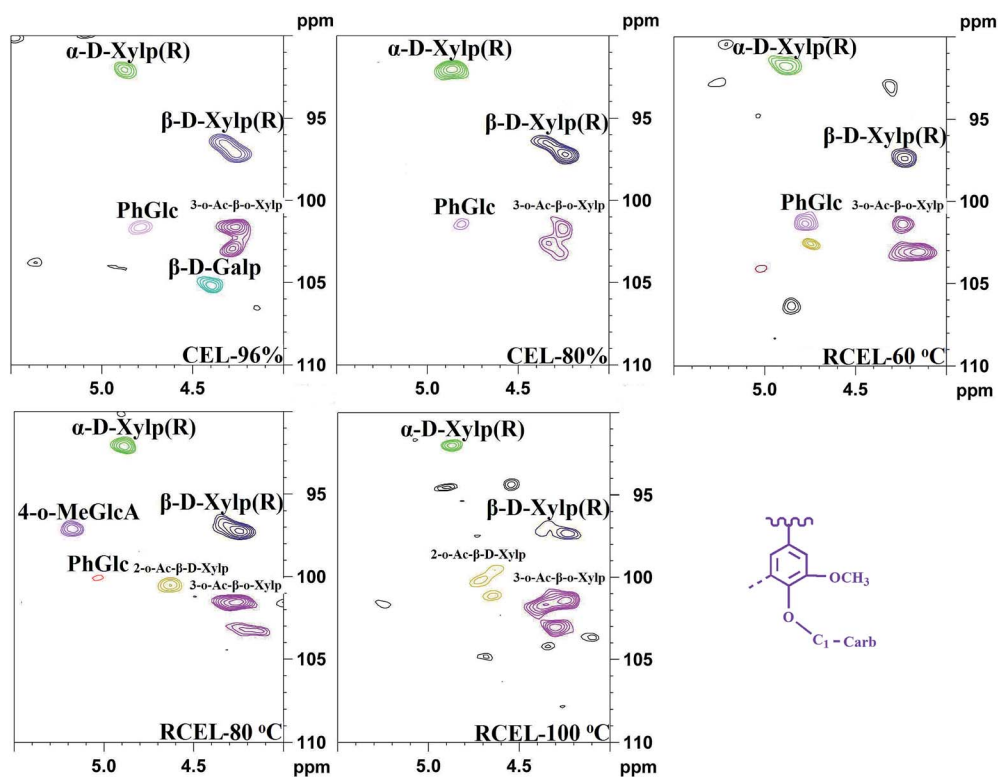


Fig. 7 2D-HSQC spectra of the lignin fractions isolated from poplar wood (anomeric regions of polysaccharides).



Table 5 Quantification of the lignin fractions by quantitative ^{31}P -NMR method (mmol g^{-1})

Sample	Aliphatic OH	Syringyl OH	Guaiacyl OH		H-Type lignin OH (PB + H) ^c	Carboxylic group
			C ^a	NC ^b		
CEL-96%	4.33	0.45	0.08	0.32	0.40	0.33
CEL-80%	3.84	0.29	0.04	0.20	0.28	1.50
RCEL-60 °C	3.57	0.33	0.07	0.24	0.30	1.16
RCEL-80 °C	4.08	0.39	0.06	0.21	0.26	1.00
RCEL-100 °C	3.46	0.23	0.03	0.17	0.23	0.88

^a C, condensed. ^b NC, non-condensed. ^c H-Type lignin phenolic OH contains *p*-hydroxybenzoate OH and *p*-hydroxyphenyl OH.

of the lignin-carbohydrates complex (LCC) linkage, such as benzyl ether (BE), decreased in RCEL-80 °C and RCEL-100 °C, suggesting that these BE bonds were cleaved gradually during the dissolution and regeneration process. In fact, low content of BE content in lignin was mostly related to the high enzymatic hydrolysis of the substrate.³⁵ Oxidation ratio of S-type lignin can be also calculated according to the ratio of $S'/(S' + S)$. It was observed that RCEL-80 °C showed the lowest oxidation ratio among these lignin samples, implying that the S-type lignin units of RCEL-80 °C were less affected by the dissolution and regeneration process. Moreover, the slight decreased PB and H_{2,6} contents also suggested that the RCEL samples were less affected by the dissolution and regeneration. Considering the yield, the contents of typical linkages β -O-4', β - β' , β -5', β -1', BE, and PB contents, it was concluded that RCEL-80 °C was excellent sample for analyzing the chemical composition and molecular structure of lignin from poplar wood.

3.7. Quantitative ^{31}P -NMR spectra

To further evaluate the functional groups of lignin samples, CEL and RCEL were comparatively investigated by quantitative ^{31}P -NMR spectrometry (Fig. S2†). The aliphatic hydroxyls, condensed and uncondensed phenolic hydroxyls, and carboxylic acids were determined by phosphitylation of the lignins with 2-chloro-4,4,5,5-tetramethyl-1,3,2-dioxaphospholane.³⁶⁻³⁹ Quantification was carried out *via* peak integration using cyclohexanol as an internal standard. Details of quantitative data, which demonstrated the various OH groups of the five lignin fractions, are listed in Table 5. It was found that the S- and G-type phenolic OH groups in CEL-80% were lower than those in CEL-96%, suggesting that the phenolic OHs in CEL-80% are occupied *via* forming some lignin-carbohydrate complex (LCC), as also reflected by aforementioned carbohydrates analysis of these CEL samples. After dissolution and regeneration process, the S- and G-type phenolic OH groups in RCEL-60 °C and RECL-80 °C increased while those for RCEL-100 °C decreased as compared to those of CEL-80%. This fact implied that dissolution under the mild temperatures (60 °C and 80 °C) resulted in the increase of the phenolic OH groups, while the declined contents of phenolic OH groups in RCEL-100 °C suggested that the released phenolic OH probably recondensed into other structures, however, this spectrum still needs to be further verified. In fact, the condensed structures of lignin can be revealed by the appearance of

condensed S_{2,6} correlated signals in the spectrum of RCEL-100 °C. Moreover, it is worth noting that the phenolic OH in H-type lignin structures (PB and H unit) characterized herein mainly belonged to *p*-hydroxybenzoate (PB) substructures specifically linked to the lignin fractions. By contrast, the content of phenolic OH in *p*-hydroxyphenyl unit was less and stable in all the lignin samples, as revealed by the aforementioned 2D-HSQC spectra. As compared to relative high content (0.40 mmol g^{-1}) of PB phenolic OH (be deemed as PB content) in CEL-96%, the decreased content (0.28 mmol g^{-1}) of PB phenolic OH was observed in CEL-80%, suggesting that different concentrations of aqueous dioxane probably affect the extraction of lignin with different phenol hydroxyl groups, which is also related to the rule of "like dissolve like". Similarly, a previous publication also demonstrated that MWL and CEL (extracted with 96% dioxane) have much higher phenolic unit contents.⁴⁰ Additionally, the slightly decreased content of PB phenolic OH in RCEL-100 °C implied that slight cleavage of PB in these lignins occurred during the relative higher dissolution temperature. However, the optimal dissolution temperature of DMSO/[Emin]OAc is 80 °C under the conditions given in this study. Furthermore, it was observed that the content of COOH groups in CEL-96% was 0.33 mmol g^{-1} , while the value increased to 1.50 mmol g^{-1} in CEL-80%. After dissolution and regeneration, the COOH contents in RCEL-60, 80 and 100 °C were 1.16, 1.00, and 0.88 mmol g^{-1} , respectively. The largely increased COOH contents in CEL-80% and RCEL-80% are mainly attributable to the existence of uronic acid in these lignins, as aforementioned (Table 2). In short, ^{31}P -NMR data indicated that the RCEL-80 °C had moderate amounts of functional groups among these lignins, suggesting the dissolution process at 80 °C is more suitable for dissolving the plant cell wall and changing the spatial structure for enzymatic attack during dissolution and regeneration process.

4. Conclusions

In the present study, a novel CEL extracting procedure was proposed based on DMSO/[Emin]OAc dissolution and regeneration process, which could significantly enhance enzymatic digestion of the regenerated substrates and extracting yield of lignin macromolecules from triploid of *Populus tomentosa* Carr. The state-of-the-art NMR techniques showed that the



dissolution/regeneration process enhanced the cleavage of lignin-carbohydrates complex and thus increasing the enzymatic hydrolysis efficiency of the regenerated substrates. In fact, the morphological changes of lignin and structural changes of carbohydrates in plant cell wall, respectively reflected by Confocal Raman Microscopy and CP-MAS NMR, leading to the enhanced enzymatic hydrolysis efficiency. Moreover, the frequencies of the major lignin linkages (β -O-4', β - β' , β -5', and β -1') and linked molecules (*p*-hydroxybenzoate) were quantitatively compared and less structural differences were observed between RCEL and CEL samples from poplar wood, indicating the applicability of this proposed method for lignin extraction is admirable. It is believed that the proposed method for lignin isolation and indentified structures of the native lignin will facilitate the effective deconstruction of the typical poplar wood. Furthermore, the representative lignin sample (RCEL) can be used as a "model lignin" to investigate the chemical transformations of lignin macromolecules in different pretreatment process under the current biorefinery process.

Acknowledgements

We are grateful for the financial support of this research from the National Natural Science Foundation of China (31500486, 31430092, 31670587), and China Ministry of Education "111" project.

References

- 1 P. Alvira, E. Tomás-Pejó, M. Ballesteros and M. Negro, *Bioresour. Technol.*, 2010, **101**(13), 4851–4861.
- 2 S.-Y. Ding, Y.-S. Liu, Y. Zeng, M. E. Himmel, J. O. Baker and E. A. Bayer, *Science*, 2012, **338**, 1055–1060.
- 3 J. Ralph, K. Lundquist, G. Brunow, F. Lu, H. Kim, P. F. Schatz, J. M. Marita, R. D. Hatfield, S. A. Ralph and J. H. Christensen, *Phytochem. Rev.*, 2004, **3**, 29–60.
- 4 Z. Strassberger, S. Tanase and G. Rothenberg, *RSC Adv.*, 2014, **4**, 25310–25318.
- 5 J. Ralph, *Chapter 6-Lignin*, Elsevier B.V., 2010.
- 6 H. Kim, J. Ralph and T. Akiyama, *BioEnergy Res.*, 2008, **1**, 56–66.
- 7 A. Björkman, *Sven. Papperstidn.*, 1956, **59**, 477–485.
- 8 H.-m. Chang, E. B. Cowling and W. Brown, *Holzforschung*, 1975, **29**, 153–159.
- 9 T.-Q. Yuan, W. Wang, F. Xu and R.-C. Sun, *Bioresour. Technol.*, 2013, **144**, 429–434.
- 10 J.-Y. Chen, Y. Shimizu, M. Takai and J. Hayashi, *Wood Sci. Technol.*, 1995, **29**, 295–306.
- 11 A. Zhang, F. Lu, R.-C. Sun and J. Ralph, *J. Agric. Food Chem.*, 2010, **58**, 3446–3450.
- 12 E. Capanema, M. Balakshin, R. Katahira, H.-m. Chang and H. Jameel, *J. Wood Chem. Technol.*, 2014, **35**, 17–26.
- 13 F. Gu, W. Wu, Z. Wang, T. Yokoyama, Y. Jin and Y. Matsumoto, *Ind. Crops Prod.*, 2015, **74**, 703–711.
- 14 K. Cheng, H. Sorek, H. Zimmermann, D. E. Wemmer and M. Pauly, *Anal. Chem.*, 2013, **85**, 3213–3221.
- 15 T.-Q. Yuan, S.-N. Sun, F. Xu and R.-C. Sun, *J. Agric. Food Chem.*, 2011, **59**, 6605–6615.
- 16 A. Sluiter, B. Hames, R. Ruiz, C. Scarlata, J. Sluiter, D. Templeton and D. Crocker, *Laboratory analytical procedure*, 2008, p. 1617.
- 17 J.-L. Wen, B.-L. Xue, F. Xu, R.-C. Sun and A. Pinkert, *Ind. Crops Prod.*, 2013, **42**, 332–343.
- 18 H.-Y. Li, S.-N. Sun, C.-Z. Wang and R.-C. Sun, *Ind. Crops Prod.*, 2015, **74**, 200–208.
- 19 J.-L. Wen, S.-L. Sun, B.-L. Xue and R.-C. Sun, *J. Agric. Food Chem.*, 2013, **61**, 635–645.
- 20 C. Crestini and D. S. Argyropoulos, *J. Agric. Food Chem.*, 1997, **45**, 1212–1219.
- 21 V. Arantes and J. N. Saddler, *Biotechnol. Biofuels*, 2010, **3**, 1–11.
- 22 X. Zhao, L. Zhang and D. Liu, *Biofuels, Bioprod. Biorefin.*, 2012, **6**, 465–482.
- 23 J. Y. Chen, Y. Shimizu, M. Takai and J. Hayashi, *Wood Sci. Technol.*, 1995, **29**, 295–306.
- 24 D. Min, H. Jameel, H. Chang, L. Lucia, Z. Wang and Y. Jin, *RSC Adv.*, 2014, **4**, 10845–10850.
- 25 G. Cheng, M. S. Kent, L. He, P. Varanasi, D. Dibble, R. Arora, K. Deng, K. Hong, Y. B. Melnichenko and B. A. Simmons, *Langmuir*, 2012, **28**, 11850–11857.
- 26 J.-L. Wen, S.-L. Sun, B.-L. Xue and R.-C. Sun, *Materials*, 2013, **6**, 359–391.
- 27 J.-L. Wen, T.-Q. Yuan, S.-L. Sun, F. Xu and R.-C. Sun, *Green Chem.*, 2014, **16**, 181–190.
- 28 J. Rencoret, G. Marques, A. Gutierrez, D. Ibarra, J. Li, G. Gellerstedt, J. I. Santos, J. Jimenez-Barbero, A. T. Martinez and J. C. del Rio, *Holzforschung*, 2008, **62**, 514–526.
- 29 J. Ralph and F. Lu, *J. Agric. Food Chem.*, 1998, **46**, 4616–4619.
- 30 K. Morreel, J. Ralph, H. Kim, F. Lu, G. Goeminne, S. Ralph, E. Messens and W. Boerjan, *Plant Physiol.*, 2004, **136**, 3537–3549.
- 31 H. Kim and J. Ralph, *Org. Biomol. Chem.*, 2010, **8**, 576–591.
- 32 M. Sette, R. Wechselberger and C. Crestini, *Chem.-Eur. J.*, 2011, **17**, 9529–9535.
- 33 Z. Hu, T.-F. Yeh, H.-m. Chang, Y. Matsumoto and J. F. Kadla, *Holzforschung*, 2006, **60**, 389–397.
- 34 P. Whiting and D. Goring, *Wood Sci. Technol.*, 1982, **16**, 261–267.
- 35 D.-y. Min, C. Yang, V. Chiang, H. Jameel and H.-m. Chang, *Fuel*, 2014, **116**, 56–62.
- 36 A. Granata and D. S. Argyropoulos, *J. Agric. Food Chem.*, 1995, **43**, 1538–1544.
- 37 D. S. Argyropoulos, *J. Wood Chem. Technol.*, 1994, **14**, 45–63.
- 38 L. G. Akim, D. S. Argyropoulos, L. Jouanin, J. C. Leplé, G. Pilate, B. Pollet, C. Lapierre, L. G. Akim, L. Jouanin and G. Pilate, *Holzforschung*, 2001, **55**, 386–390.
- 39 A. Jääskeläinen, Y. Sun, D. Argyropoulos, T. Tamminen and B. Hortling, *Wood Sci. Technol.*, 2003, **37**, 91–102.
- 40 T. Ikeda, K. Holtman, J. F. Kadla, H.-m. Chang and H. Jameel, *J. Agric. Food Chem.*, 2002, **50**, 129–135.

